Journal of Physics: Conference Series **507** (2014) 042008 doi:10.1088/1742-6596/507/4/042008

HTS ion damage Josephson junction technology for SQUID arrays

S Ouanani[1], J Kermorvant[2], D-G Crété[1], Y Lemaître[1], J-C Mage[1], B Marcilhac[1], N Bergeal[3], M Malnou[3], J Lesueur[3], D Mailly[4], C Ulysse[4]

[1]Unité Mixte de Physique CNRS/Thales and Université Paris-Sud, 1 Av. A Fresnel, FR-91767 Palaiseau, France
[2]THALES Communication and Security, 4 Av. des Louvresses, 92622 Gennevilliers CEDEx, France
[3]LPEM / ESPCI-CNRS-UPMC, 10 Rue Vauquelin, FR-75005 Paris, France
[4]Laboratoire de Photonique et de Nanostructures, Route de Nozay FR-91460 Marcoussis, France

denis.crete@thalesgroup.com

Abstract. The high temperature superconducting (HTS) Josephson Junction (JJ) ion damage technology we are developing is well suited for making large SQUID arrays. We have studied arrays of similar SQUIDs together with large SQIFs (Superconducting Quantum Interference Filter) with 2000 SQUIDs of different loop areas. Magnetic field sensitivity has been measured in both types of devices as a function of bias current and temperature. The effects of the barrier thickness (from 20 to 80 nm) and JJ length (2 or 5 µm) on characteristics have been investigated.

1. Introduction

SQUIDs (Superconducting Quantum Interference Device) made with low critical temperature (T_c) superconductors are known as the most sensitive magnetic sensors and have been used in a wide range of applications [1]. High critical temperature (HTc) devices, as they operate at higher temperature, can expand further the domain of application, provided they have comparable performance. One way to improve the sensitivity and the dynamic range is to create SQUID arrays, either with similar areas or with a random distribution of hole sizes. For such multiple-loop configuration named SQIFs (Superconducting Quantum Interference Filters), the magnetic flux to voltage transfer function shows a unique dip around zero magnetic flux. Therefore, SQIFs can be used to measure absolute magnetic field. Besides, their sensitivity and dynamic range are expected to increase as $N^{1/2}$ [2].

In this paper, we present experimental results on SQUID arrays produced by ion damage technology on $YBa_2Cu_3O_7$ (YBCO) thin films. Two kinds of arrays were investigated: arrays of N identical SQUIDs in series with N=1, 5, 12 and 22 and a series-array of 2000 SQUIDs with pseudo-random distribution of hole sizes from 6 to 60 µm^2.

2. Fabrication Method

The process, already described in [3, 4], is briefly be summarized here. A 150 nm thick c-axis oriented YBCO film was thermally coevaporated on a sapphire substrate [5] and then covered by an in situ 100 nm thick gold layer. After Ar-ion beam etching of the gold contact layer, a photoresist is patterned to protect superconducting strips from subsequent irradiation with 110 keV oxygen ions at large fluence to make the unprotected YBCO insulating. A PMMA (polymethylmethacrylate) resist is then deposited all over the sample, and a very narrow (20-nm wide) slit is opened across each arm of the superconducting loop by electron beam lithography. A second 110 keV oxygen ion irradiation performed at smaller fluence defines the junction barrier. This technique allows one to make controllable and reproducible Josephson junctions [6] and SQUIDs [7].

3. Experimental Results

3.1. Identical SQUID arrays

Arrays used in this study are made of 64 identical SQUIDs of 30 μm^2 square loop areas connected in series, with intermediate contacts to test several series of 1, 5, 12 and 22 SQUIDs. The JJ geometry has been varied from array to array: three barrier thickness (20, 40 and 80 nm) and two JJ lengths (2 and 5 µm) have been used. The arm width was maintained at 5 µm.

We define the parameter T_j as the highest temperature for Josephson coupling. All arrays have T_j ~74-76 K, depending on the barrier thickness (see below), with a slightly higher value for a single SQUID. The current-voltage characteristics are RSJ-like [1] at moderate bias currents.

Figure 1 shows the output voltage V across one single SQUID with JJ length of 2 µm and barrier thickness of 40 nm, versus applied magnetic field for several values of the dc bias current between 0.9 I_c and 1.15 I_c (fig. 1). For I_{bias}=340 µA (~1.04 I_c), the amplitude is maximum with a peak to peak output voltage of 13 µV. The period for one SQUID is 130 mG, corresponding to an effective area of ~130 μm^2 which has been evaluated around 85 μm^2: this enhancement is presumably due to a flux-focusing effect caused by a nearby superconducting plane [7]. In addition to the SQUID modulations, the characteristic Fraunhofer pattern associated with the junctions themselves is observed (not shown here). This behaviour demonstrates the high quality of the junctions.

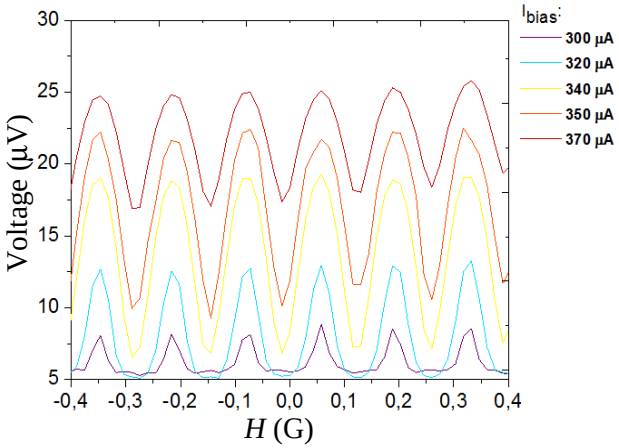

Figure 1: Voltage V vs. applied magnetic field H for a single SQUID at different bias currents.

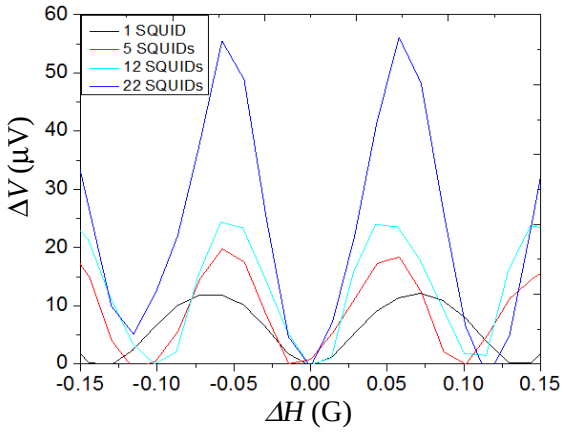

Figure 2: Voltage vs. magnetic field for 4 N-series arrays with N = 1, 5, 12 and 22 SQUIDs. Curves are shifted both horizontally and vertically for easier comparison.

The amplitude of the modulation increases with N, the number of SQUIDs in series, but not linearly as expected (see fig. 2) [8]. Non-uniformity in the magnetic environment may create destructive interferences and therefore, a decrease of the modulation amplitude. Also, as seen from the field period, the field focusing factor is not the same for all arrays, due to the different embedding superconducting circuit.

3.2. SQIF

Figure 3 presents the voltage response as a function of the applied magnetic field for a series array of 2000 SQUIDs with randomly distributed loop areas between 6 and 60 µm^2 and JJ geometry 40 nm × 2 µm (at T= 73 K and I_{bias}= 40 µA).

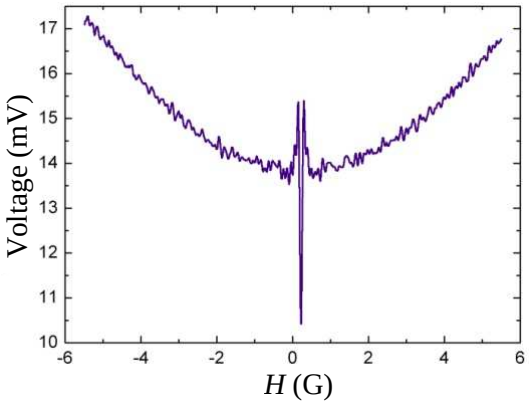

Figure 3: The voltage vs external magnetic field transfer function of a SQIF shows a unique delta-peak around B = 0.

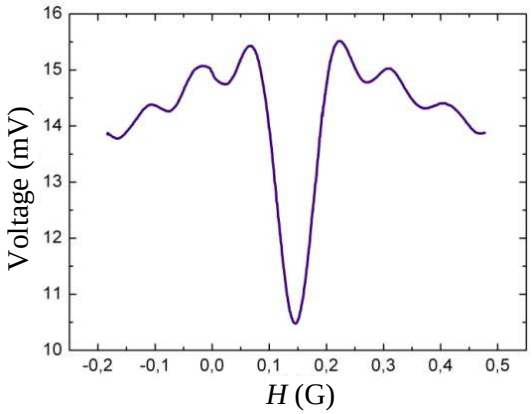

Figure 4: Enlarged central peak showing residual SQUID oscillations and offset of about 0.15 G.

As expected [2], an aperiodic $V(H)$ response is observed and characterized by a single sharp dip centred near zero magnetic field. In addition, the parabolic background seen in fig. 3 is due to the response of the JJs to the magnetic field and residual SQUID oscillations are also visible on both sides of the dip (cf. fig 4). One can note the slight shift in the peak position regarding to the zero field value due to the ambient magnetic flux trapping during the cooling down of the sample. The amplitude of the voltage swing and the slope dV/dH of the linear part of the SQIF dip strongly depend on both operating temperature and bias current (fig. 5 & 6). We find the optimal SQIF modulation conditions to be T = 73 K which is 0.8 K lower than T_j and I_{bias}= 40 µA which is 0.5 µA higher than the corresponding critical current of the whole structure. The maximum voltage is 5 mV and the transfer factor is equal to 105 mV.G^{-1}.

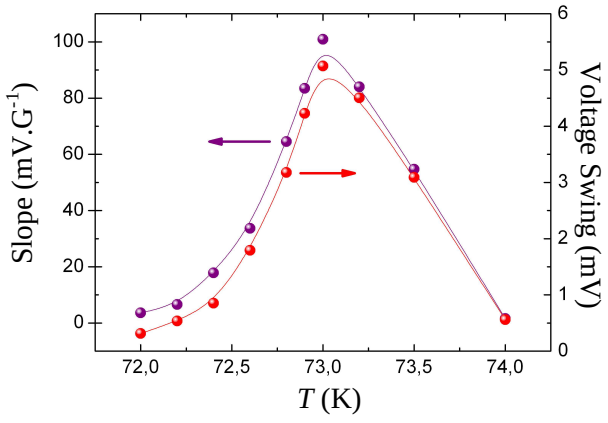

Figure 5: Evolution of the transfer factor and the voltage swing vs. T at I_{bias} = 35 µA. Lines are guides to the eye.

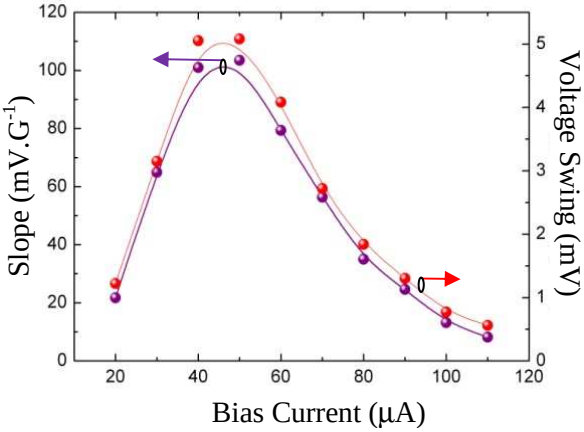

Figure 6: Evolution of the transfer factor and the voltage swing vs. I_{bias} at T = 73 K. Lines are guides to the eye.

3.3. Influence of the barrier thickness

To illustrate the scaling of barrier properties with thickness t_B, we report on the resistance R measured at a given temperature for a given probe current I_{probe}. Experimentally, R is measured versus T using I_{probe}= 10 µA, for series arrays on a 2 µm wide microbridge with t_B= 20, 40 and 80 nm.

We define T_i as the temperature at which the resistance vanishes, i.e. $I_c(T_i) \sim I_{probe}$, and $R_{Plateau}$, the resistance at midpoint of the plateau between T_i and the critical temperature T_c. The dependences of T_i

and $R_{Plateau}$ as a function of t_B are shown fig. 7: as expected, T_i decreases (solid line) and $R_{Plateau}$ increases (dashed line), with the barrier thickness. Linear extrapolation of $R_{Plateau}(t_B)$ at $R_{Plateau}$= 0 Ω defines an "excess barrier thickness" t_{eb} of the order of 88 nm. Because the resistance depends only weakly on temperature in the range of the plateau, and because the $V(I)$ curve is linear in this range, this result very weakly depends on the arbitrary choice of I_{probe}. It indicates some straggling of the damaged area, as proposed by Wolf [9]: the irradiated material can be regarded as a superconductor whose local critical temperature and critical current density are reduced depending on the local defect density and induces a bias-current dependence of the normal resistance (visible at large bias currents). In order to investigate further the transport properties in the barrier area, we have also used $V(I)$ measurements at various temperatures, to apply the above procedure and produce the graph on fig. 8, t_{eb} versus T and I. Here, the ratio $V(I,T)/I$ has been substituted for $R_{Plateau}$. It shows that the excess barrier thickness increases with both current and temperature: again this is in qualitative agreement with the effect of local defect density which is the highest in the barrier region facing the aperture of the mask, and decreases as the distance to the barrier region increases.

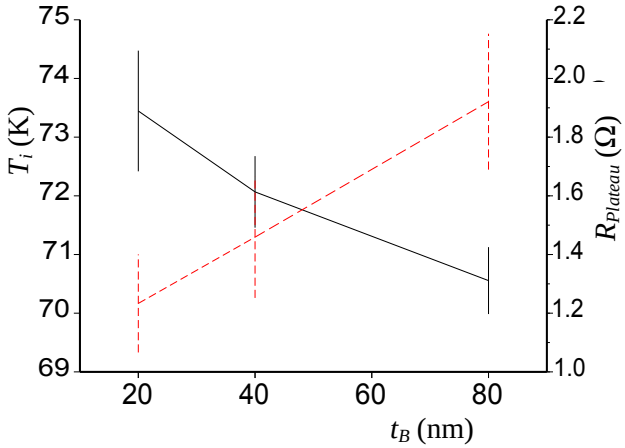

Figure 7 : Variations of T_i, the temperature at which I_c=10 µA (solid line), and $R_{Plateau}$, the device resistance at $(T_i+T_c)/2$ (dashed line), for 3 values of the nominal barrier thickness t_B. Vertical bars are 1-σ scattering over a dozen of devices.

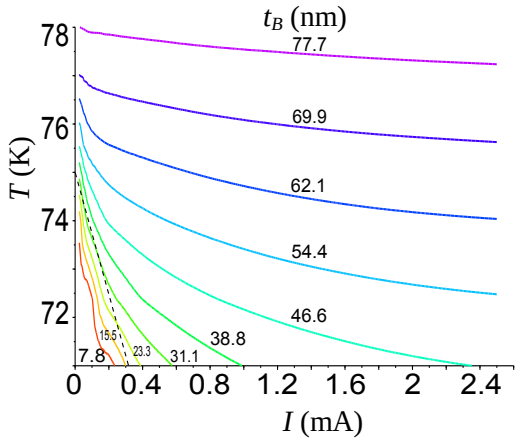

Figure 8 : Contour plot of the excess barrier thickness t_{eb} (labelled in nm) versus T and I. The lower left part of the diagram delimited by the dashed line is the region where I becomes comparable to $I_c(T)$.

4. Conclusion

Ion damage technology is a successful method to achieve large SQUID arrays. Results on SQIF are very promising and need to be investigated more deeply. Noise measurements to characterize the sensitivity of single SQUID and SQIFs have to be done in a close future.

References

[1] SQUID Handbook, J. Clarke and A.I. Braginski Eds., 2004 Wiley-VCH
[2] J. Oppenländer *et al*., 2001 *IEEE Trans Appl. Supercond.* **Vol. 11**, pp.1271-1274
[3] S. Ouanani *et al*., 2013 jul.7-12, *IEEE, Intern. Supercond. Electron. Conf.*, Cambridge, Ma. http://ieeexplore.ieee.org/stamp/stamp.jsp?tp=&arnumber=6604297
[4] N. Bergeal *et al*., 2007 *J. Appl. Phys.* **102**, 083903
[5] http://www.ceraco.de/
[6] N. Bergeal *et al*., 2005 *Appl. Phys. Lett.* **87**, 102502
[7] N. Bergeal *et al*., 2006 *Appl. Phys. Lett.* **89**, 112515
[8] K. Li *et al*., 1995 *IEEE, Trans. Appl. Supercond.*, **Vol 5**, pp.3255-3258
[9] T. Wolf, 2011 PhD dissertation : « Etude de nanojonctions Josephson à haute température critique en vue d'application terahertz » Université P& M. Curie, Paris